Coastal Research Library 14

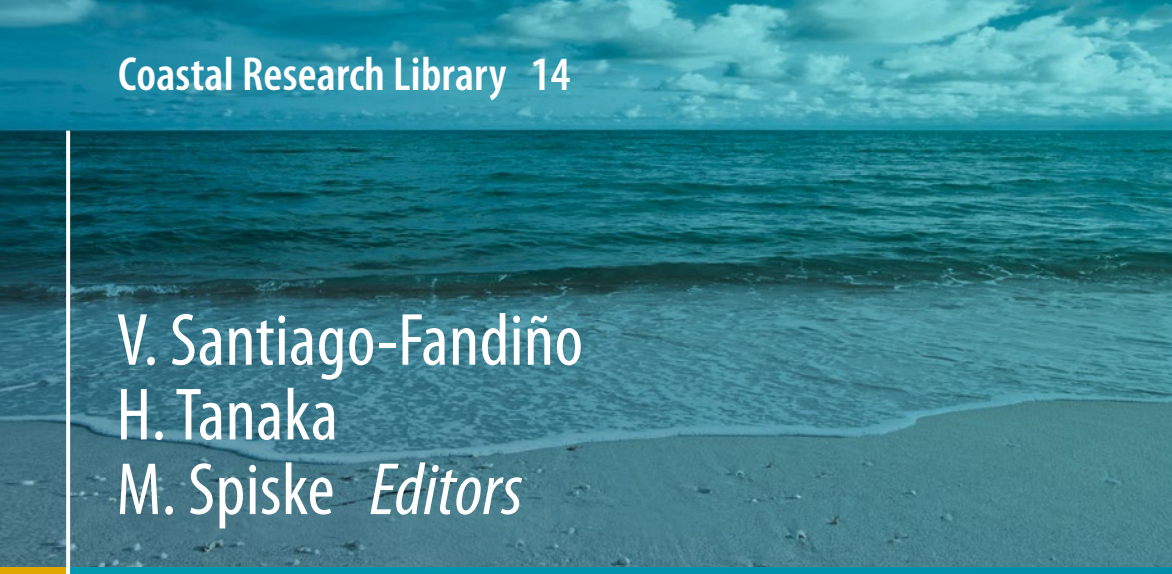

V. Santiago-Fandiño
H. Tanaka
M. Spiske *Editors*

Tsunamis and Earthquakes in Coastal Environments

Significance and Restoration

Springer

Coastal Research Library

Volume 14

Series Editor

Charles W. Finkl
Department of Geosciences
Florida Atlantic University
Boca Raton, FL
USA

The aim of this book series is to disseminate information to the coastal research community. The Series covers all aspects of coastal research including but not limited to relevant aspects of geological sciences, biology (incl. ecology and coastal marine ecosystems), geomorphology (physical geography), climate, littoral oceanography, coastal hydraulics, environmental (resource) management, engineering, and remote sensing. Policy, coastal law, and relevant issues such as conflict resolution and risk management would also be covered by the Series. The scope of the Series is broad and with a unique cross-disciplinary nature. The Series would tend to focus on topics that are of current interest and which carry some import as opposed to traditional titles that are esoteric and non-controversial. Monographs as well as contributed volumes are welcomed.

More information about this series at http://www.springer.com/series/8795

V. Santiago-Fandiño • H. Tanaka • M. Spiske
Editors

Tsunamis and Earthquakes in Coastal Environments

Significance and Restoration

Springer

Editors
V. Santiago-Fandiño
Villaviciosa, Asturias, Spain

M. Spiske
Department of Geology and Paleontology
Westfälische Wilhelms-University
Münster, Germany

H. Tanaka
Department of Civil Engineering
Tohoku University
Sendai, Japan

ISSN 2211-0577 ISSN 2211-0585 (electronic)
Coastal Research Library
ISBN 978-3-319-28526-9 ISBN 978-3-319-28528-3 (eBook)
DOI 10.1007/978-3-319-28528-3

Library of Congress Control Number: 2016937980

Printed on acid-free paper

This Springer imprint is published by Springer Nature
The registered company is Springer International Publishing AG Switzerland

Foreword

Coastal zones are valuable areas where sea, land, and atmosphere meet. They are characterized by coastal topography and nearshore waves which drive various dynamic processes to interact with each other. The coastal topography serves as the basis of the environment, in which waves will break and produce turbulent mixing, dissipating wave energy and providing a wealthy coastal zone utilized by many ecosystems for various activities. In the coastal zone, vigorous sediment movement due to nearshore waves continuously changes the topography which protects land from flooding. Coastal environments based on coastal topography are therefore important in coastal hazard mitigation as well as sustainability of society. However, coastal environments are highly variable in broad timescales from minutes to decades, affected by natural and anthropogenic impacts from both the ocean and the land.

Coastal erosion is accelerating on many coasts all over the world. Water pollution and eutrophication are degrading coastal environments in semi-enclosed bays backed by megacities. Understanding the cumulative impact of these types of environmental degradation is difficult since the transport of sediment and nutrients is affected not only by waves, currents, and topography in the coastal zone but also by various inland natural and anthropogenic changes that lead to the increase and decrease of materials delivered to the coast. The impact is sometimes rapid urbanization far from the coastal zone. The response is sometimes delayed as long as several decades.

Large tsunamis and earthquakes are infrequent natural events capable of causing large-scale destruction along coastal areas by heavily altering their physical and environmental characteristics. Although coastlines are naturally highly dynamic systems, these events cause dramatic changes in estuaries, coastal lagoons, tidal flats, wetlands, and beaches resulting in large alterations in their morphology, sediment, depth, water quality, surface area, and flow, as well as inhibiting flora and fauna in a very short period of time. On occasion, the impact is so large that these coastal features even disappear completely.

History abounds with examples of devastating tsunamis that originated from different causes, most commonly from earthquakes. The first record of a Holocene

tsunami is related to the Storegga slide, a large submarine landslide in the North Sea around 6000 BC, which heavily impacted the coastline of Norway as sediment was found up to 20 m above sea level. In modern-day history, there are more than 50 records of large tsunamis and related earthquakes, including the most recent events in the Indian and Pacific Oceans (2004 Sumatra, 2010 Chile, and 2011 Japan).

In terms of human life, NOAA states that since 1850, about 420,000 lives have been lost due to tsunamis as local coastal communities and large villages, towns, and even cities have been impacted. Likewise, losses in infrastructure, the economy, and ecosystem services have amounted to trillions of dollars.

Tsunamis like the 2004 Indian Ocean Tsunami and the 2011 Tohoku Tsunami caused catastrophic damage to coastal areas. Many reconstruction processes are being introduced in the affected areas including structure-based countermeasures and nonstructure-based relocation and evacuation plans. In consideration of accelerating reconstruction processes, we need to pay deliberate attention to long-term treatment of coastal environments.

Restoration and reconstruction of damaged areas are the cause of large debates; on one side, arguments for the paramount importance of human protection at all costs, without proper consideration of the environment, have prevailed, while on the other, there are increased calls for a more balanced approach to harmonize measures of protection with the environment in order to allow coastal ecosystems to thrive. The restoration process and reconstruction measures in certain countries could be taken as an example of both, but unfortunately aesthetic and visual restoration is often mistaken for full environmental restoration.

This book deals with impacts of tsunamis and earthquakes on coastal environments. In addition to direct impact and response due to flooding and abrasion, the text covers physical, chemical, and biological responses in coastal morphology, water quality, and ecosystems. Comprehensive descriptions of multi-scale impacts of tsunami and earthquake events, both spatially and temporally, will help us to understand the complicated interactions developed in coastal zones and to achieve the sustainable resilient environment and society with smart post-event recovery. I believe this book will be beneficial to researchers and students in science and engineering as well as policy-makers, urban planning engineers, and coastal managers.

The University of Tokyo Shinji Sato
Tokyo, Japan

Acknowledgments

The editors would like to express deep appreciation to the authors of the chapters of this book for their most valuable contributions. Their collaboration is an example of of dedication and motivation toward the development of science and knowledge as well as sharing of information in the field of tsunami and earthquakes in coastal areas. Likewise, gratitude is also due to the reviewers for their most valuable comments and suggestions and, last but not least, to all others who in one form or another have contributed to the production of this book.

Contents

Contributors

Iftikhar Ahmed Abbasi Department of Earth Science, College of Science, Sultan Qaboos University, Muscat, Sultanate of Oman

Mohammad Bagus Adityawan Water Resources Engineering Research Group, Institut Teknologi Bandung, Bandung, Indonesia

Department of Civil Engineering, Tohoku University, Sendai, Japan

Bruno Adriano Graduate School of Engineering, Tohoku University, Aramaki, Aoba-ku, Sendai, Japan

C. Andrade IDL and Departamento de Geologia, Faculdade de Ciências da Universidade de Lisboa, Lisboa, Portugal

Ram Avtar Institute for the Advance Study of Sustainability (UNU-IAS), United Nations University, Tokyo, Japan

P.J.M. Costa IDL and Departamento de Geologia, Faculdade de Ciências da Universidade de Lisboa, Lisboa, Portugal

N.P. Dissanayaka Institute of Oceanography, University Malaysia Terengganu (UMT), Kuala Terengganu, Malaysia

Jie Dou Graduate School of Frontier Science, The University of Tokyo, Kashiwa, Japan

Miguel Estrada Centro Peruano Japonés de Investigaciones Sísmicas y Mitigación de Desastres (CISMID), Universidad Nacional de Ingeniería, Lima, Peru

M.C. Freitas IDL and Departamento de Geologia, Faculdade de Ciências da Universidade de Lisboa, Lisboa, Portugal

Yushiro Fujii International Institute of Seismology and Earthquake Engineering (IISEE), Building Research Institute (BRI), Tsukuba, Ibaraki, Japan

R. González-Villanueva Dpto. Xeociencias Mariñas e O.T. (XM-1), Facultade de Ciencias do Mar Universidade de Vigo, Campus As Lagoas Marcosende, Vigo, Pontevedra, Spain

Kenji Harada Center for Integrated Research and Education of Natural Hazards, Shizuoka University, Shizuoka, Japan

Vo Cong Hoang Department of Civil Engineering, Tohoku University, Sendai, Japan

Thuyloi University - Southern Campus, Ho Chi Minh, Vietnam

Kinuko Ito Graduate School of Agricultural Science, Tohoku University, Aobaku, Sendai, Japan

L.P. Jayatissa Department of Botany, University of Ruhuna, Matara, Sri Lanka

Din Mohammed Kakar Department of Geology, Baluchistan University, Quetta, Baluchistan, Pakistan

Ayu Katayama Graduate School of Agricultural Science, Tohoku University, Aobaku, Sendai, Japan

Mohammed Asif Khan Karakorum International University, Gilgit, Pakistan

Naoko Kimura Department of Sustainable Rural Development, Graduate School of Global Environmental Studies, Kyoto University, Kyoto, Japan

K.A.S. Kodikara Department of Botany, University of Ruhuna, Matara, Sri Lanka

Widjo Kongko Coastal Dynamics Research Center, BPPT, Jakarta, Indonesia

Shunichi Koshimura International Research Institute of Disaster Science (IRIDeS), Tohoku University, Aramaki, Aoba-ku, Sendai, Japan

Akira Mano International Research Institute of Disaster Science, Tohoku University, Sendai, Japan

Erick Mas International Research Institute of Disaster Science (IRIDeS), Tohoku University, Aramaki, Aoba-ku, Sendai, Japan

Antonio Mascarenhas CSIR-National Institute of Oceanography, Goa, India

Hideo Matsutomi Department of Civil Engineering, Akita University, Akita, Japan

Yuta Mitobe Department of Civil Engineering, Tohoku University, Sendai, Japan

Norihiro Monna Graduate School of Agricultural Science, Tohoku University, Aobaku, Sendai, Japan

Abdul Muhari Directorate for Coastal and Ocean, Ministry of Marine Affairs and Fisheries, Republic of Indonesia, Jakarta, Indonesia

A.C. Narayana Centre for Earth & Space Sciences, University of Hyderabad, Hyderabad, India

Osamu Nishimura Department of Civil and Environmental Engineering, Tohoku University, Sendai, Japan

M.A. Oliveira IDL and Departamento de Geologia, Faculdade de Ciências da Universidade de Lisboa, Lisboa, Portugal

Min Roh Department of Civil Engineering, Tohoku University, Sendai, Japan

Eko Rudianto Directorate for Coastal and Ocean, Ministry of Marine Affairs and Fisheries, Republic of Indonesia, Jakarta, Indonesia

Enggar Sadtopo Directorate for Coastal and Ocean, Ministry of Marine Affairs and Fisheries, Republic of Indonesia, Jakarta, Indonesia

Takashi Sakamaki International Research Institute of Disaster Science, Tohoku University, Sendai, Japan

Department of Civil and Environmental Engineering, Tohoku University, Sendai, Japan

Youhei Sakurai Department of Civil and Environmental Engineering, Tohoku University, Sendai, Japan

Ahmed Sana Department of Civil Engineering, College of Engineering, Sultan Qaboos University, Muscat, Sultanate of Oman

Vicente Santiago-Fandiño Environmental Advisor, Villaviciosa, Asturias, Spain

B. Satyanarayana Institute of Oceanography, University Malaysia Terengganu (UMT), Kuala Terengganu, Malaysia

Jaya Kumar Seelam CSIR-National Institute of Oceanography, Goa, India

Kazunori Shizuka Graduate School of Agricultural Science, Tohoku University, Aobaku, Sendai, Japan

Hendra Yusran Siry Directorate for Coastal and Ocean, Ministry of Marine Affairs and Fisheries, Republic of Indonesia, Jakarta, Indonesia

Yuriko Takeda International Research Institute of Disaster Science, Tohoku University, Sendai, Japan

Hitoshi Tanaka Department of Civil and Environmental Engineering, Tohoku University, Sendai, Japan

Kaoru Tojo Department of Civil and Environmental Engineering, Tohoku University, Sendai, Japan

Keiko Udo International Research Institute of Disaster Science, Tohoku University, Sendai, Japan

Hideaki Yanagisawa Department of Regional Management, Faculty of Liberal Arts, Tohoku Gakuin University, Izumi-ku, Sendai, Miyagi, Japan

Ali P. Yunus Graduate School of Frontier Science, The University of Tokyo, Kashiwa, Japan

Chapter 1
Revisiting the 2001 Peruvian Earthquake and Tsunami Impact Along Camana Beach and the Coastline Using Numerical Modeling and Satellite Imaging

Bruno Adriano, Erick Mas, Shunichi Koshimura, Yushiro Fujii, Hideaki Yanagisawa, and Miguel Estrada

Abstract On June 23, 2001, a moment magnitude Mw 8.4 earthquake occurred off the southern coast of Peru causing substantial damage to urban and agricultural areas. The tsunami generated by this earthquake reached up to 7 m run-up height and extended over 1.3 km inundation. This paper aims to revisit the impact of the 2001 Peruvian tsunami on the coastal area and its morphology along Camana city. The tsunami source is reconstructed through inversion of tsunami waveform records observed at several tide gauge stations and the impact is analyzed using the numerical result and moderate-resolution satellite images to calculate the inundation features in the coast. Finally we propose the tsunami source model suitable for further analysis of this event through tsunami numerical simulations. In addition,

B. Adriano (✉)
Graduate School of Engineering, Tohoku University,
Aoba 468-1-E301, Aramaki, Aoba-ku, Sendai 980-0845, Japan
e-mail: adriano@geoinfo.civil.tohoku.ac.jp

E. Mas • S. Koshimura
International Research Institute of Disaster Science (IRIDeS), Tohoku University,
Aoba 468-1-E302, Aramaki, Aoba-ku, Sendai 980-0845, Japan
e-mail: mas@irides.tohoku.ac.jp; koshimura@irides.tohoku.ac.jp

Y. Fujii
International Institute of Seismology and Earthquake Engineering (IISEE), Building Research Institute (BRI), 1 Tachihara, Tsukuba, Ibaraki 305-0802, Japan
e-mail: fujii@kenken.go.jp

H. Yanagisawa
Department of Regional Management, Faculty of Liberal Arts, Tohoku Gakuin University,
2-1-1 Tenjinzawa, Izumi-ku, Sendai, Miyagi 981-3193, Japan
e-mail: h-yanagi@izcc.tohoku-gakuin.ac.jp

M. Estrada
Centro Peruano Japonés de Investigaciones Sísmicas y Mitigación de Desastres (CISMID),
Universidad Nacional de Ingeniería, Av. Túpac Amaru No. 1150 – Lima 25 Apartado
Postal 31-250 Lima 31, Lima, Peru
e-mail: estrada@uni.edu.pe

V. Santiago-Fandiño et al. (eds.), *Tsunamis and Earthquakes in Coastal Environments*, Coastal Research Library 14, DOI 10.1007/978-3-319-28528-3_1

environmental changes, in particular the impact to vegetation areas, were evaluated using satellite imagery. An important reduction of agricultural areas due to tsunami impact and soil salinization was confirmed.

Keywords Peru earthquake • Tsunami source • Inversion • Modeling • Remote sensing

1.1 Introduction

The tsunami generated by the 23 June 2001 Peru Earthquake (M_w 8.4) generated a destructive tsunami that struck the southern region of the Peruvian coast. The post-tsunami survey team (ITST: International Tsunami Survey Team) reported tsunami heights, distance of inundation and structural damage (ITST 2001a, b, c). ITST reported that the destruction due to the tsunami was mainly concentrated in Camana along 30 km of a sandy populated beach. The average value of run-up height was 5 m with a maximum value of 7 m. The inundation distance reached between 700 m and 1.3 km inland. As a result, the agricultural fields in the Camana estuary were covered with up to 40 cm of sand deposits (Okal et al. 2002). Official records estimated that at least 57 people were killed by the earthquake and 26 by the tsunami, while 2812 were injured and approximately 60,000 houses were damaged or destroyed (MINSA/OPS 2005). An engineering analysis of the recorded ground motion conducted by Rodriguez-Marek et al. (2010) shows that the earthquake presented peak ground accelerations between 0.04 and 0.34 g for distances from the fault between 70 and 220 km. Within the framework of the project Enhancement of Earthquake and Tsunami Disaster Mitigation Technology in Peru (JST-JICA SATREPS) (Yamazaki et al. 2013), Peruvian and Japanese research teams had conducted field surveys in the affected areas of Camana which remain unreconstructed since 2001. They had found tsunami traces, such as watermarks on walls, still present in remaining destroyed buildings of the urban area to the south of Camana beach (Shoji et al. 2014; Yanagisawa et al. 2011). Furthermore, Spiske et al. (2013) analyzed the changes of tsunami deposits after 7 years from the main event, and found that approximately 25 % of the original sediment layer had been reduced during this period.

The seismological discussion of the 2001 Peru earthquake, including the tsunami impact, had been addressed in detail on several scientific publications (e.g., Audemard et al. 2005; Bilek 2002; Giovanni 2002; Okal et al. 2002; Tavera et al. 2002, 2006). However, few studies had focused on reproducing the tsunami inundation (Adriano et al. 2011; Jimenez et al. 2011). Therefore, in this study, the main purpose is to reproduce, through numerical modeling and satellite image analysis, the tsunami impact of this event to the Camana beach coastline and its morphology. The following discussion is divided in three sections. First, a seismic source model estimated from tsunami data is introduced; this source is suitable for modeling tsunami inundation. The proposed source model is based on tsunami waveform inversion of recorded signals at several tide gauge stations. In the second section, using the calculated seismic source, a non-lineal tsunami numerical modeling is conducted to reproduce

the inundation area, the maximum inundation depth, and the tsunami run-up. Finally, in the third section, the tsunami impact to Camana beach coastline is evaluated using the tsunami numerical results and pre- and post-event satellite images.

1.1.1 Developing the Tsunami Source Model

1.1.1.1 Seismic Source Models

The 2001 Peru earthquake occurred on June 23 (15:33:14 local time) along the Peru-Chile trench. The main shock took place at the subduction zone between Nazca and South American plates. The Nazca plate is sub-ducting underneath of the South American plate at a rate of 4.3–4.5 cm/year (Fig. 1.1). This inter-plate contact zone is the longest and one of the most active plate boundaries worldwide (Audemard

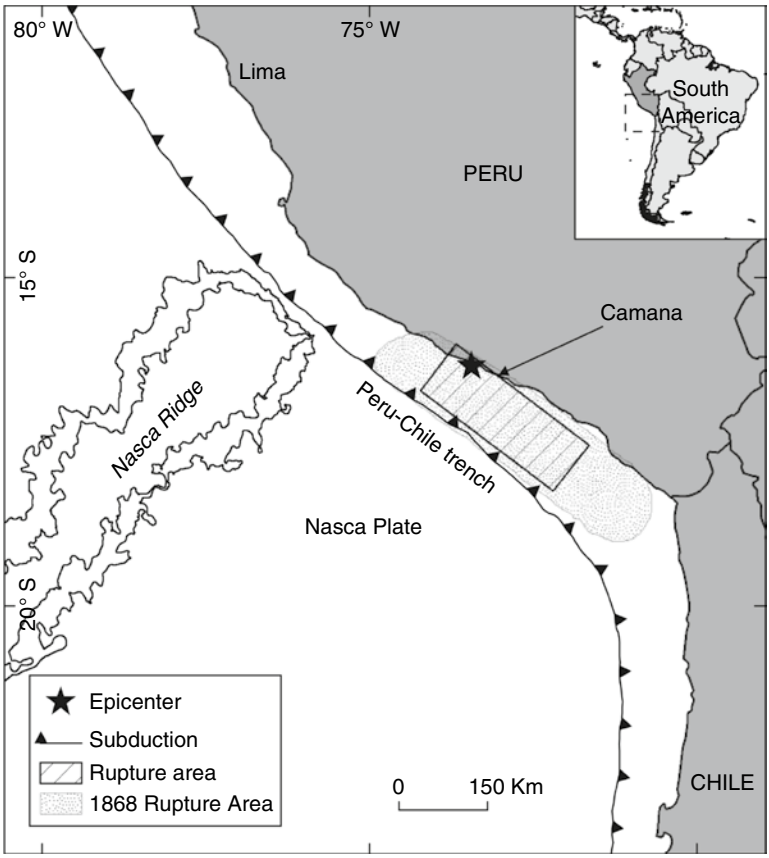

Fig. 1.1 Tectonic setting of southern Peru and northern Chile. The epicenter and rupture area of the 2001 event are shown by the *black star* and the hatched polygon, respectively

et al. 2005) and it has generated several large and catastrophic earthquakes in the past (Dorbath et al. 1990).

The epicenter of the 2001 event was located at 73.64°W 16.26°S (USGS) while the hypocenter was estimated at 73.94 ± 2.5 km west and 16.46 ± 3.9 km south with 30.4 ± 9.5 km depth according to the Geophysical Institute of Peru (IGP) (Tavera et al. 2002; Ocola 2008). Based on the Modified Mercalli Intensity scale the maximum intensity of ground shaking was VII (Tavera et al. 2006). The rupture process duration was estimated by the Global CMT catalog as 86 s and by Kikuchi and Yamanaka (2001) as 107 s. The estimated magnitude varied from M_w 8.2 to M_w 8.4. For instance, Kikuchi and Yamanaka (2001) analyzed teleseismic broadband *P* waves retrieved from 24 seismic stations to determine the general source parameters. They estimated a moment magnitude of M_w 8.2 and a seismic moment of 2.2×10^{21} Nm in a rupture area of 150 km × 240 km. Similarly, Tavera et al. (2002) determined the fault plane orientation and magnitude of Mw 8.2 by analyzing the polarity of *P* waves and body waveform inversion from 15 broadband stations at teleseismic distances. Another analysis of *P* waveforms from 14-recorded seismograms estimated a total seismic moment of 2.4×10^{21} Nm, which gives a moment magnitude of M_w 8.2 (Giovanni 2002). Conversely, the Global CMT catalog reported a seismic moment of 4.7×10^{21} Nm with a moment magnitude of M_w 8.4. This event was followed by intensive aftershock sequences of approximately 400 earthquakes during the first month after the earthquake. The strongest aftershock was on July 7, 2001 with a moment magnitude M_w 7.5 (Bilek 2002; Tavera et al. 2006).

Most of the earthquake source models that have been proposed for the 2001 Peru earthquake are based on the observation and the analysis of seismic data. Conversely, this study contributes on presenting a source model calculated from tsunami waveform inversion as a follow-up estimation from a previous source proposed by Adriano et al. (2012) but using new bathymetry data available and different tide gauges in the area for better approximation.

1.1.1.2 Tsunami Data

The 23 June 2001 Peru tsunami was recorded in several tide gauge stations around the Pacific Ocean (Goring 2002). In this study the tide gauge data were taken from the National Oceanic and Atmospheric Administration (NOAA)/Pacific Marine Environmental Laboratory (PMEL), Center for Tsunami Research, which were provided by the National Oceanic Services (NOS)/NOAA, Field Operation Division, Pacific Regional Office. These data were originally sampled in 1-min and 15-s intervals. According to NOS/NOAA, the data had a minimal editing/reformatting and no quality controls were performed.

For this event, we used tsunami waves recorded at eight tide gauge stations located in Chile and one station located in Peru (Fig. 1.2a). We retrieved the tsunami signal by approximating the tidal wave as a polynomial function and remove it from the original record. Then, the initial time of the earthquake (T_0 = 2001/06/23

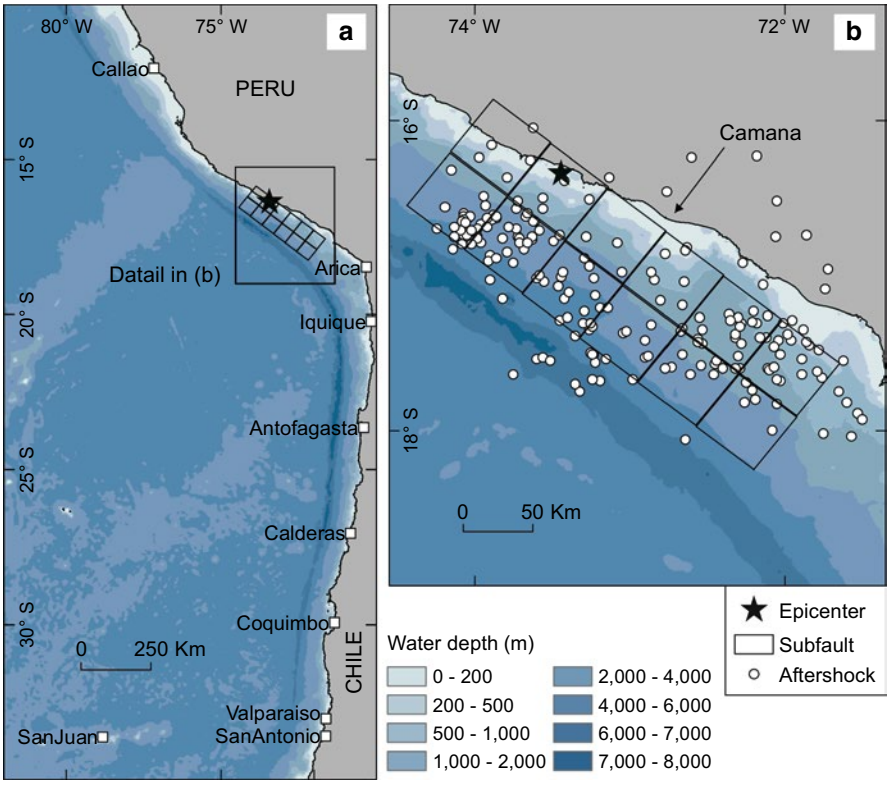

Fig. 1.2 (**a**) Location of the tide gauge stations used for the tsunami waveform inversion (*solid white square*). (**b**) Inferred fault geometry of the 2001 Peru Earthquake from aftershocks distribution

20:33:14 UTC, according to USGS) was subtracted. Finally, the tsunami waveforms were resampled in 1-min interval for tsunami inversion, as shown by red dashed lines in Fig. 1.3.

1.1.1.3 Tsunami Waveform Inversion

The focal parameters of the earthquake source are based on the Global CMT catalog (strike 308°, dip 18°, slip angle 63°). Figure 1.2b shows the epicenter and the extent of aftershocks over a 7-day window following the main-shock. Based on the aftershock distribution a 300 km in length and 100 km width area was set as the rupture zone oriented southeast from the epicenter. In addition, the fault area was divided in 12 subfaults (50 km × 50 km) to cover the aftershock area as shown in Fig. 1.2b. The top depths of subfaults are 14.15 km and 29.60 km southwest northeast from the trench to the coast.

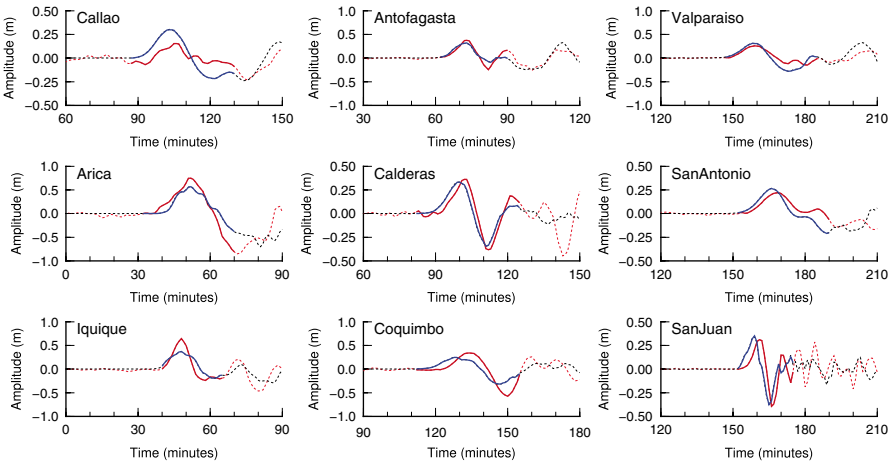

Fig. 1.3 Comparison of the recorded (*red*) and synthetic (*blue*) tsunami waveforms computed from the estimated slip distribution. The time intervals shown in solid lines were used for the inversion; *dashed lines* are shown only for comparison but those were not use in the source model estimation

To calculate the synthetic tsunami waveform at the tide gauge stations, tsunami propagation from each subfault to the stations was calculated using the linear shallow-water approximation (Satake 1995). The computational domain is shown in Fig. 1.2a. The bathymetry data was constructed from the General Bathymetry Chart of the Ocean (GEBCO) 30 arc-seconds grid data. As the initial condition, static deformation of the seafloor is calculated for a rectangular fault model (Okada 1985). In addition, the effect of coseismic horizontal displacement was also included (Tanioka and Satake 1996). The non-negative least square method was used to estimate the slip distribution. The details of the inversion method are described in Fujii and Satake (2007). The calculation of later phases or reflected waves in the tsunami signal is particularly difficult and inaccurate with the coarse resolution in the bathymetry data; therefore, only the first cycle of tsunami waveform was used for the inversion process.

The comparison of the recorded (red curves) and synthetic (blue curves) tsunami waveforms computed from the estimated slip distribution is shown in Fig. 1.3. In general, the synthetic waveforms agree with the observed data at stations located far from the source. Conversely, there is a 15 cm difference on the estimated maximum amplitude at Callao station. Although the maximum amplitude of Callao, Arica, and Iquique stations is not well reproduced, the phases are well estimated. The inversion results are shown in Table 1.1 and Fig. 1.4a. The total seismic moment was calculated from the slip distribution as 4.07×10^{21} Nm (M_w 8.3) using 4.0×10^{10} N/m^2 as average rigidity value in an elastic medium. The inversion result indicates that the maximum slip corresponds to the deepest subfaults (No. 9–10), near Camana beach. The land-level changes calculated from the slip distribution suggest a coastal subsidence of approximately 1.07 m near Camana beach (Fig. 1.4b) while GPS measurements estimated 0.84 cm of land subsidence at Camana (Ocola 2008).

Table 1.1 Earthquake source model obtained from the tsunami waveform inversion

No.	Strike angle (°)	Dip angle (°)	Rake angle (°)	Length (km)	Width (km)	Slip (m)	Depth (km)	Lat. (°)	Lon. (°)
1	308	18	63	50	50	0.05	14.15	−18.25°	−72.20
2	308	18	63	50	50	0.00	14.15	−17.97	−72.58
3	308	18	63	50	50	2.34	14.15	−17.68	−72.95
4	308	18	63	50	50	0.00	14.15	−17.40	−73.32
5	308	18	63	50	50	0.00	14.15	−17.12	−73.69
6	308	18	63	50	50	0.00	14.15	−16.83	−74.07
7	308	18	63	50	50	0.00	29.60	−17.90	−71.92
8	308	18	63	50	50	1.73	29.60	−17.62	−72.30
9	308	18	63	50	50	10.18	29.60	−17.33	−72.67
10	308	18	63	50	50	10.94	29.60	−17.05	−73.04
11	308	18	63	50	50	7.32	29.60	−16.76	−73.41
12	308	18	63	50	50	0.00	29.60	−16.48	−73.79

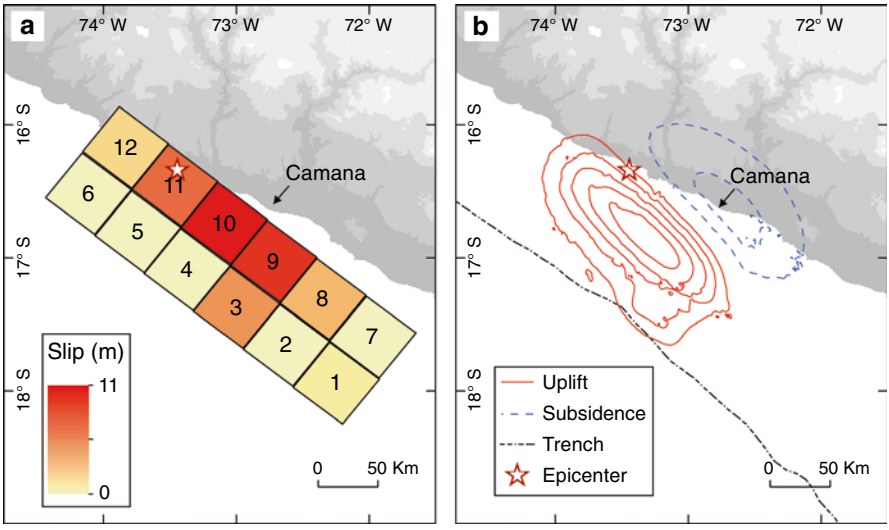

Fig. 1.4 (**a**) Slip distributions estimated by tsunami waveform inversion. The color scale shows the slip value for each subfault. The star shows the epicenter. (**b**) Seafloor deformation computed from the estimated slip distribution. The *red solid contours* indicate uplift with a contour interval of 0.5 m, whereas the *blue dashed contours* indicate subsidence, with a contour interval of 0.5 m

1.1.2 Numerical Simulation of Tsunami Inundation

1.1.2.1 Numerical Model Set-Up

The Tohoku University's Numerical Analysis Model for Investigation of Near-Field Tsunami No.2 (TUNAMI-N2) model, which is based on the non-linear shallow

water approximation, was used to conduct the tsunami numerical simulation. A set of non-linear shallow water equations (1.1, 1.2 and 1.33) are discretized by the Staggered Leap-frog finite difference scheme (Imamura 1996). The bottom friction coefficients in the Manning's equation are set according to the land use (Table 1.1).

$$\frac{\partial \eta}{\partial t} + \frac{\partial M}{\partial x} + \frac{\partial N}{\partial Y} = 0 \tag{1.1}$$

$$\frac{\partial M}{\partial t} + \frac{\partial}{\partial x}\left(\frac{M^2}{D}\right) + \frac{\partial}{\partial y}\left(\frac{MN}{D}\right) = -gD\frac{\partial \eta}{\partial x} - \frac{gn^2}{D^{7/3}}\mathrm{M}\sqrt{M^2+N^2} \tag{1.2}$$

$$\frac{\partial N}{\partial t} + \frac{\partial}{\partial x}\left(\frac{MN}{D}\right) + \frac{\partial}{\partial y}\left(\frac{N^2}{D}\right) = -gD\frac{\partial \eta}{\partial y} - \frac{gn^2}{D^{7/3}}\mathrm{N}\sqrt{M^2+N^2} \tag{1.3}$$

where

$$M = \int_{\eta}^{-h} u dz \tag{1.4}$$

$$N = \int_{\eta}^{-h} v dz \tag{1.5}$$

$$D = \eta + h \tag{1.6}$$

M and N are the discharge flux of x and y direction, respectively, η is the water level and h is the water depth above the mean sea level.

The computational domain is divided into four subdomains to construct a nested grid system, as shown in Fig. 1.5. The grid size, which extends from the earthquake source region to the coast of Camana coast, varies from 30 to 810 m. The bathymetry data for the first to the third domains were interpolated from the GEBCO 30 arc-seconds grid data. The merged topography and bathymetry grids for the fourth domain were constructed from the nautical chart provided by the DHN, Navy of Peru (Dirección de Hidrografía y Navegación in Spanish) and the land elevation data obtained from the Thermal Emission and Reflection Radiometer (ASTER) sensor with 1 arc-second grid resolution.

For the tsunami inundation model, the land resistance during tsunami penetration is considered by setting a specific roughness coefficient to the land cover (Table 1.2) (Aburaya and Imamura 2002; Dutta et al. 2007; Kotani et al. 1998). Figure 1.6 shows the spatial distribution of Manning's roughness coefficient (n) in the computational domain of tsunami inundation model. The n-distribution was obtained through the unsupervised classification of moderate resolution satellite image. In addition, the coastline of Camana beach and surroundings were estimated from the analysis of satellite images. The detail of this step is discussed in Sect. 1.4.1.

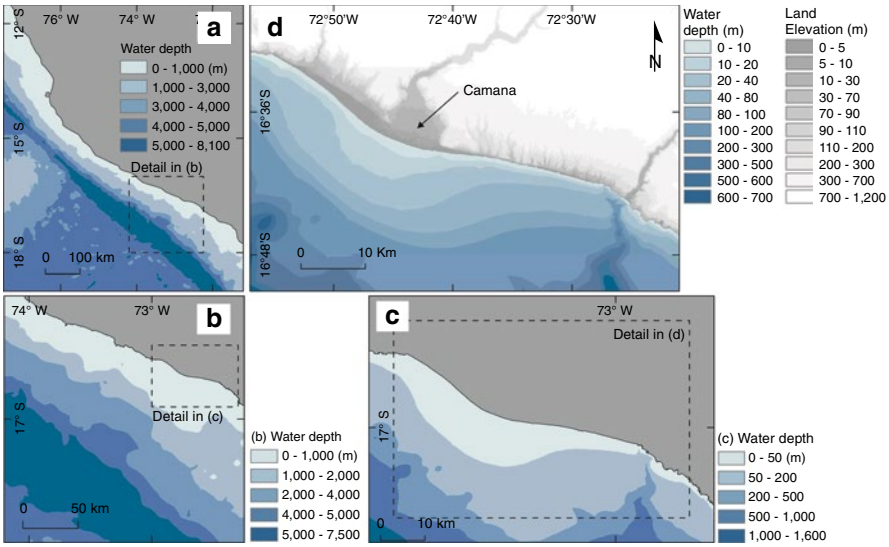

Fig. 1.5 The computational domain for the model of tsunami propagation and inundation to the coastal area of Camana city. The grid size varies from 810, 270, 90 to 30 m, as shown in the nested grid system detailed by (**a**–**d**)

Table 1.2 Manning's roughness coefficient (*n*) values according to (Kotani et al. 1998)

Smooth ground	0.020
Shallow water area or natural beach	0.025
Vegetated area	0.030
Populated area	0.040

1.1.2.2 Results and Validation of Tsunami Inundation Model in Camana Coast

As shown in Fig. 1.5, the topography in Camana coast is predominantly of low lands penetrating as much as 1.0 km. Following the plain beach area, steep hills can be observed in the north and south from the river mouth (Fig. 1.5d). This topography gives a natural barrier against the tsunami penetration. According to the satellite imagery analysis, almost 5 km inland from the coastline of Camana beach is used for agriculture. In addition, based on the model results, the tsunami penetrated 1.0–1.5 km inland in this area.

Results from simulation were validated through the comparison with field surveyed inundation data. Figure 1.7 shows the spatial distribution of modeled maximum tsunami inundation depths. The maximum inundation depth in the computational domain is 8.5 m. The tsunami penetration at Playa Pucchun and south of Camana beach (La Punta – Las Cuevas) agrees with the observed data (ITST 2001a, b, c; Dengler 2001). It was observed that the urban area located to the south of Camana beach, between the La Punta and the Las Cuevas, was inundated

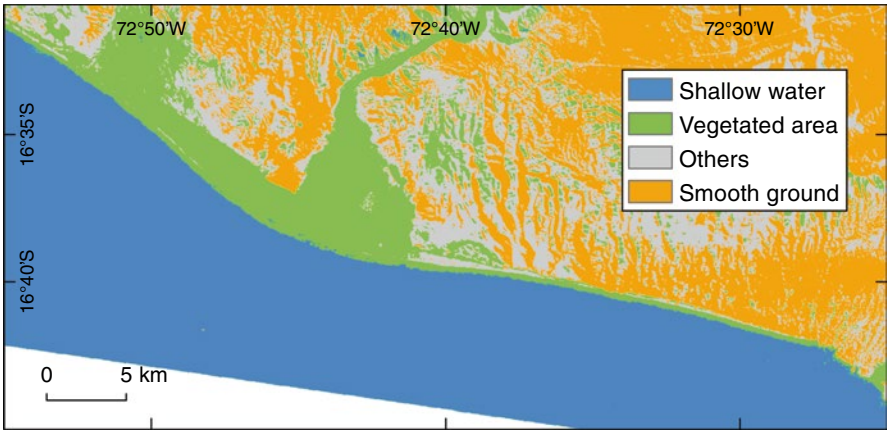

Fig. 1.6 Spatial distribution of roughness coefficient, according to the land-use condition, inferred from the unsupervised classification of pre-tsunami satellite imagery (Landsat-5 TM)

with 3–4 m (Fig. 1.7d). On the other hand, the agricultural areas to the north of Camana beach were inundated with 2–3 m (Fig. 1.7b, c). Except for areas in the north of Camana beach (Playa la Chira), where the calculated tsunami penetration slightly overestimates the limits observed by the ITST 2001 survey, simulation results are consistent with in-situ measurement data. Discrepancies in the north part of Camana are due to the limitation of the shallow water approximation added to the lack of local bathymetry information within the study area, in particular near the Playa La Chira.

The modeled tsunami inundation is validated by K and κ coefficients proposed by Aida (1978) According to the ITST 2001 survey, 20 points of local inundation depth were measured around Camana beach (Fig. 1.7a). Figure 1.8 shows a lineal comparison of simulated and measured tsunami inundation depth. Based on the suggested guidelines provided by JSCE (2002) ($0.95 < K < 1.05$ and $\kappa < 1.45$), our results can be evaluated as suitable ($K = 1.02$ and $\kappa < 1.07$) to be used for evaluating tsunami impact along Camana beach coastline and its morphology.

1.1.3 Impact of the Tsunami Inundation in Camana Coast

1.1.3.1 Method

Satellite images were selected based on its acquisition time and free-cloud coverage in the study area. Unfortunately there was no available image acquired within a short time after or before the tsunami event. Nevertheless, we selected three Landsat-5 Thematic Mapper (TM) images scenes (Path 04, Row 71; according to the World Reference System 2). Two pre-event images taken on June 21, 1999, almost 2 years before the event, and on June 10, 2001, almost 2 week before the